
SHISHULM: LIGHTWEIGHT LANGUAGE MODEL WITH HYBRID DECODER-MLP ARCHITECTURE AND PAIRED WEIGHT SHARING

Shivanshu Kumar¹ Gopalakrishnan Srinivasan¹

ABSTRACT

While the transformer architecture has achieved state-of-the-art performance on natural language processing tasks, these models impose substantial memory and computational overhead. Recent research has identified significant architectural redundancies within these models, presenting opportunities for optimization without compromising performance. Taking insights from research in AI interpretability and inference-time layer pruning, we introduce an efficient language model architecture, referred to as ShishuLM, which reduces both the parameter count and Key-Value (KV) cache requirements. Given the increasing importance of Small Language Models (SLMs) in agentic AI systems, we evaluate our approach on two SLMs of different scales. Our analysis reveals that for moderate-context scenarios, normalization coupled with attention computation is roughly linear with the input, enabling entire transformer blocks to be approximated through Multi-Layer Perceptrons (MLPs). Our results show that ShishuLM provides up to 25% reduction in memory requirements and up to 40% improvement in latency during both training and inference, compared to parent models. Our experimental and analytical findings provide insights towards building more efficient SLM architectures from a pre-training standpoint.

1 INTRODUCTION

The transformer architecture, introduced by (Vaswani et al., 2017), has demonstrated state-of-the-art performance in various sequence modeling and vision tasks. Its superior performance is attributed to the combination of attention mechanism along with residual connections (Siddiqui et al., 2024). Large Language Models (LLMs) typically contain billions of trainable parameters (Bai et al., 2023; Touvron et al., 2023; Jiang et al., 2023; Javaheripi et al., 2023). The sheer number of model parameters necessitates substantial memory solely for storage. During training, memory requirements escalate further since backpropagation requires storing intermediate activations. Additionally, the size of the KV cache grows with longer input sequences and larger model sizes, compounding the issue.

In this regard, prior research has attempted to improve the memory and computational efficiency of LLMs by identifying and eliminating redundancies in the transformer architecture. For example, various structured and unstructured pruning methods have been proposed to remove superfluous parameters (Ma et al., 2023; Frantar & Alistarh, 2023). Furthermore, some studies have adopted layer pruning strategies by quantifying the importance of different layers using metrics like cosine similarity between the inputs and outputs

of transformer blocks (Men et al., 2024; Yang et al., 2024b; Gromov et al., 2025), Shapley-value based metrics (Siddiqui et al., 2024), and perplexity measured on a calibration set (Song et al., 2024). For instance, in decoder-only models using the LLaMA architecture, the later layers exhibit high similarity between their inputs and outputs and are thus categorized as less important (Men et al., 2024; Gromov et al., 2025). The resulting sub-model offers improved computational efficiency while maintaining performance comparable to the original model.

A separate line of research focuses on reducing the Key-Value (KV) cache requirements by pre-training models with the key-value pairs shared across different layers. Wu & Tu compute keys and values only at a later layer and share them across bottom layers, whereas Sun et al. compute key-value pairs only for the first half of the layers and share them across the remaining layers. This too reveals redundancy in attention computation in the later transformer blocks.

Furthermore, research on AI interpretability has advocated for a layer-wise evolution of the token representation. Lad et al. show that tokens go through different stages of processing and the “work” done by each layer is depth-dependent, hypothesizing four universal stages of inference. Artzy & Schwartz study the specific roles of the attention layers at different depths, showing that previous token dependency is prominent in the initial layers and that information is highly dependent on the attention mechanism. Later layers are responsible for consolidation and internal processing,

¹Department of Computer Science and Engineering, Indian Institute of Technology, Madras. Correspondence to: Shivanshu Kumar <cs23b058@smail.iitm.ac.in>, Gopalakrishnan Srinivasan <sgopal@cse.iitm.ac.in>.

where the model becomes less sensitive to manipulations of previous token representations.

Building on these insights, we ask the following question:

Can we still maintain performance while fully utilizing the parameters of the model?

Our experiments indicate that retaining complete decoder blocks for up to one-third of the total number of layers, while removing attention layers from the remaining blocks results in models with negligible performance loss. Although this significantly reduces KV cache storage, a large number of parameters still reside in the MLP layers. To address this, we share the weights across adjacent layers by analyzing weight distributions in existing pre-trained models (Touvron et al., 2023; Liu et al., 2024). In addition, we quantify the approximate linearity of attention modules for moderate-sized contexts and mathematically establish the sufficiency of an MLP layer to perform the equivalent computation of an entire block.

To the best of our knowledge, this is one of the first works to combine insights from interpretability research to enhance model efficiency. We believe that our work will help pave a new line of research in this direction. Our key contributions are as follows.

1. We propose ShishuLM¹, an efficient architecture for pre-training decoder-only transformer-based language models, which employs only MLP layers in the later blocks of the model along with weight sharing.
2. We validate ShishuLM by achieving comparable performance using two models released by Liu et al., containing 125 and 600 million parameters, with significant reduction in parameter and KV cache requirements.
3. We mathematically establish that our model is equivalent to a vanilla transformer for moderate context-settings and provide insights for identifying layer-level redundancy.

Existing optimization techniques, such as quantization (Hubara et al., 2017), multi-query attention (Ainslie et al., 2023), and grouped-query attention (Ainslie et al., 2023) are orthogonal to our approach and can be applied to our models for further optimization.

2 RELATED WORK

In this section, we review related techniques proposed to optimize transformer models.

Pruning: Pruning involves removing redundant parameters in the model and can be performed at both the individual weight and block levels, as explained below.

1. **Weight pruning** involves removing redundant weights and avoiding the corresponding computations to achieve speed up and reduction in model size. Structured pruning involves removing entire structural components such as rows, columns, or blocks from weight matrices (Ashkboos et al., 2024; Ma et al., 2023). On the other hand, unstructured pruning removes individual weights by setting them to zero, creating sparse matrices without following predetermined structural patterns (Frantar & Alistarh, 2023; Sun et al., 2024a).

Such pruning methods typically require specialized hardware to achieve maximum benefit. For example, NVIDIA tensor cores offer support for 2:4 structured sparsity but necessitate large batch sizes to obtain meaningful gains in performance (Song et al., 2024; Mishra et al., 2021).

2. **Block pruning** involves identifying redundant blocks (decoder layers) in the network at inference time using either an importance or redundancy metric, eliminating the less important (or more redundant) layers, and subsequently fine-tuning the compressed model to recover performance. Elimination of entire blocks not only lowers parameter count but also reduces the memory overhead associated with maintaining KV cache, which scales linearly with the sequence length.

Men et al. quantify layer importance based on expected cosine similarity between the input and output of a block, and prune blocks with low scores. Gromov et al. also use cosine similarity, but remove an entire block of consecutive layers, followed by fine-tuning using Quantization and Low Rank Adapters (QLoRA). Yang et al. replace consecutive layers with a single layer by appropriately setting the parameters of the replaced layer. On the other hand, Siddiqui et al. use a Shapley value-based metric measured on a calibration dataset for quantifying block importance. Song et al. iteratively prune blocks by evaluating the perplexity on a calibration set and remove the most redundant block at each step. However, these methods retain the high costs of pre-training while incurring additional overhead for layer selection and post-training optimization.

Sub-quadratic attention: A different line of research aims to reduce the time and memory complexity of transformers by proposing various algorithmic enhancements. During auto-regressive generation, the attention mechanism exhibits quadratic computational complexity $O(T^2)$ and linear memory complexity $O(T)$ with respect to sequence length T .

¹The word "Shishu" in Sanskrit means "baby"

For each newly generated token, the query vector must compute attention scores with the key vectors of all preceding tokens, while the KV cache stores all the previous key-value pairs to avoid recomputation.

Gu & Dao use selective State Space Models (SSMs) as a fundamental alternative. Rather than treating all input tokens equally, Mamba dynamically determines which information to retain in its bounded hidden state to achieve $O(1)$ space complexity and $O(T)$ time complexity. Katharopoulos et al. introduced linear attention by expressing self-attention as a linear dot-product of kernel feature maps. Using the associativity in matrix multiplication, they remove the quadratic dependency on sequence length. They further show that linear attention is equivalent to maintaining context information in constant space. Yang et al. extended traditional linear attention by incorporating data-dependent gating mechanisms.

Despite higher efficiency, architectures with constant-size hidden state representations suffer from recency bias, where recent tokens disproportionately influence the hidden state. This makes it hard to capture long-range dependencies. Ro et al. maintain both linear and quadratic attention versions for every layer. An attention-score entropy metric dynamically decides which version to use at inference time, balancing computational cost and accuracy. However, this requires costly pre-training along with distillation to train the linear versions of each layer.

KV cache sharing: Seeking to reduce KV cache requirements, several works have attempted to share the key-value pairs across attention layers. Brandon et al. proposed sharing KV pairs across adjacent layers in groups of two, reducing the KV cache size by roughly 50%. Sun et al. also compress the KV cache by 50% by computing KV pairs only for the first half of the model and sharing them for the remaining layers. Rajput et al. place sliding window attention layers sandwiched between global attention layers, sharing keys and values across the global layers and between consecutive sliding window layers. Wu & Tu further compress the KV cache by computing keys and values only in the top layers and pairing them with queries in the bottom layers.

Interpretability and evolution of token representation:

The field of AI interpretability seeks to understand how machine learning models process information and make decisions. Lad et al. perform a depth dependent analysis on the role of different layers in decoder-only transformers. They identify four distinct stages of inference: detokenization (early layers integrate local context), feature engineering (middle layers build contextual representations), prediction ensembling (converting features to token predictions), and residual sharpening (final output refinement).

Artzy & Schwartz reveal a depth-dependent division of attention mechanisms, showing that early layers primarily use attention for gathering information from previous tokens, while the later layers shift towards internal consolidation with significantly reduced attention importance. Their findings indicate that manipulating representations in the top 30-50% of layers has minimal performance impact, supporting the hypothesis that layers serve fundamentally different computational purposes with changing depth.

3 PRELIMINARIES: EARTH MOVER’S DISTANCE

Earth Mover’s Distance (Rubner et al., 1998) or EMD, also known as the Wasserstein distance, is a metric for quantifying the dissimilarity between probability distributions by framing the comparison as an optimal transport problem. Given two distributions, EMD computes the minimum cost required to transform one distribution into another, where the cost is determined by the amount of *probability mass* that must be moved and the distance over which it must be transported.

We employ the EMD metric to study the distribution similarity of weights across layers, which are discrete.

Formally, for two discrete probability distributions $P = \{p_i\}$ and $Q = \{q_j\}$, EMD reduces to the solution of the linear programming problem specified by

$$EMD(P, Q) = \min_T \sum_{i,j} T_{ij} d_{ij},$$

subject to the following constraints.

$$\sum_j T_{ij} = p_i \forall i$$

$$\sum_i T_{ij} = q_j \forall j$$

$$T_{ij} \geq 0 \forall i, j$$

T_{ij} denotes the amount of probability mass transported from point i in P to point j in Q , and d_{ij} is the ground distance between these points (or absolute difference of values in the univariate case).

4 SHISHULM: ARCHITECTURE AND METHODOLOGY

4.1 ShishuMLP

Decoder-only transformer models consist of transformer blocks that are stacked sequentially. Please note that we use the terms “decoder layer” and “transformer blocks” interchangeably. Each of the decoder layers further consists

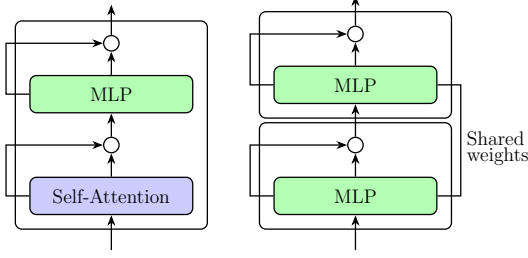


Figure 1. Vanilla transformer block(left) and a pair of consecutive ShishuMLP blocks with shared weights (right)

of a Mutli-Headed-Self-Attention (MHSA) layer followed by a Multi Layer Perceptron (MLP) layer (The inputs are normalized before passing to these layers). The MHSA and MLP layers are connected in a residual fashion, i.e., the inputs are added to the outputs before being passed to the next layer, as shown in Figure 1. Let L denote the number of decoder layers in the model, and x_i be the input to the i^{th} block. The forward computation is given by

$$x_{i+1} = y_i + \text{MLP}(\text{LN}(y_i))$$

where,

$$y_i = x_i + \text{Self-Attention}(\text{LN}(x_i)).$$

$\text{MLP}(\cdot)$, $\text{LN}(\cdot)$, and $\text{Self-Attention}(\cdot)$ represent the functions computed by MLP, normalization and self-attention layers, respectively.

In the proposed ShishuLM architecture, we introduce the ShishuMLP block, which consists of a normalization layer followed by an MLP layer. Essentially, we remove the self-attention and input normalization layers from a standard transformer block to obtain the ShishuMLP block. For an input x_i , the forward pass is computed as

$$x_{i+1} = x_i + \text{MLP}(\text{LN}(x_i)).$$

4.2 Optimization Methodology

For our lightweight ShishuLM architecture, we investigate the utility of attention layers in the deeper layers of a language model from a pre-training perspective, seeking to answer the following question:

Is there a particular "attention budget" required to maintain model performance?

To address this question, we progressively eliminate the input normalization and attention layers and measure the resulting validation and training losses. For this experiment, we use MobileLLM-125M, a 125-million parameter model based on the LLaMA architecture (Liu et al., 2024) and

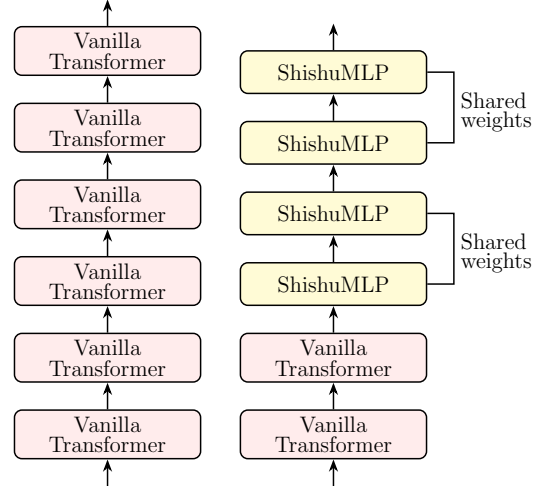


Figure 2. Schematic representation of the ShishuLM architecture as compared to the Llama architecture

pre-train it on the MiniPile (Kaddour, 2023) dataset for quick testing.

We find that up to $2/3^{rd}$ of the attention layers can be removed without much loss in performance. We empirically observe that less than $1/3^{rd}$ attention causes degradation in performance. With one-third of the attention layers, we observe that retaining most of the attention layers in the bottom blocks is helpful to maintain performance within the same attention budget. Experimental details are presented in Appendix E.

4.3 Linearity in the Attention Modules

In this section, we mathematically analyze why pre-training without attention does not affect performance through the following three steps:

1. We observe that the combined computation of the input normalization layer and self-attention is approximately linear.
2. Furthermore, this linearity takes the form αI , which essentially scales the input vectors by a constant factor.
3. Since the normalization layer reduces the variance to 1, this scaling factor is effectively eliminated, thus establishing the equivalence of the computation for the entire block.

Motivated by our experimental observation that the computation of the input normalization and self-attention layer is approximately linear, we fit a linear regression model to the corresponding sets of inputs and outputs for each layer. To

make sure that our analysis accounts for sequential token dependencies, we feed the inputs in a pre-filling manner one after the other, as explained below. Let the sequence

$$t_1, t_2, t_3 \dots t_T$$

be the input prompt to our model and let it generate up to b tokens. For the j^{th} token in the sequence ($j \in [T + b]$), let x_{ij} denote the input to the i^{th} decoder layer and z_{ij} be the output of the input normalization and self-attention layers. We find W_i satisfying

$$\min_{W_i} \sum_{j=1}^T \|W_i x_{ij} - z_{ij}\|_2^2 \quad (1)$$

For sequence lengths $T < 512$ we can fit such a W_i for every layer with negligible Mean Squared Error (MSE).

We further investigate the nature of W_i across different layers and find that, after adding the residual connection, the cosine similarity between the input and output is nearly 1 (refer Appendix C). In other words, $\forall j \in [T + b]$,

$$\frac{x_{ij}^T (W_i x_{ij} + x_{ij})}{\|x_{ij}\|_2 \cdot \|W_i x_{ij} + x_{ij}\|_2} = \frac{x_{ij}^T W_i' x_{ij}}{\|x_{ij}\|_2 \cdot \|W_i' x_{ij}\|_2} \approx 1.$$

Drawing motivation from this finding, we set $W_i'' = \alpha I$ for some $\alpha \in \mathbb{R}$ such that

$$\min_{W_i''} \|W_i'' - W_i'\|_2^2. \quad (2)$$

If we reduce our computation to an equivalent computational block that computes $W_i'' x_{ij}$ instead of $z_{ij} + x_{ij}$, we obtain that the input to the post-attention normalization layer is

$$\alpha \cdot x_{ij}$$

but,

$$LN(\alpha \cdot x_{ij}) \approx LN(x_{ij}) \quad (3)$$

(Please refer to Appendix A for a detailed Proof) Essentially, the normalization layer remains unaffected with scaling. Therefore, bypassing the computation of input normalization + self-attention layers leads to negligible impact on performance. However, this does not imply all attention modules are entirely redundant, since we are studying pre-trained models and the layer computations are not independent. This is consistent with our experiments, which show that removing attention layers beyond a certain point results in severe performance degradation. The Mean Squared Errors for Equations 1 and 2 can be found in Appendix C.

4.4 Similarity in MLP Weight Distribution

Since most of the model parameters reside in the MLP layers, as a next step, we identify parameter redundancy in these layers. We begin by analyzing the weight distributions of up, down, and gate projection matrices in the MLP layers. To further quantify similarity, we measure the Earth-Mover’s distance (Rubner et al., 1998) between weight distributions across layers. We compute the ratio of these distributions with the range of weights (for every layer) and evaluate the maximum of these ratios. Formally, if EMD_i denotes the Earth Mover’s distance between decoder layers i and $i + 1$, and Δ_i denotes the range of the weights in the i^{th} layer, we define

$$r_i = \frac{EMD_i}{\min(\Delta_i, \Delta_{i+1})}$$

and compute

$$r_{max} = \max_{i \in [L-1]} r_i.$$

Normalizing the Earth Mover’s distance with the range provides a clearer metric of similarity at scale. Lower values indicate higher similarity and vice versa. We observe greater similarity with increasing model size. Even with the parent models we choose, observed values are almost always $< 0.5\%$. The r_{max} values and distribution similarity heat maps are reported in Appendix D.

Building on these observations, we propose weight sharing across consecutive ShishuMLP layers in pairs to optimize the trade-off between computational efficiency and parameter count. This approach reduces memory overhead associated with backpropagation operations, including gradient storage, which scales directly with the number of model parameters. In summary:

1. We use standard decoder layers for first $L/3$ layers.
2. For the remaining $2L/3$ layers, we use ShishuMLP layers, sharing weights across adjacent layers in pairs of 2.

The resultant model is a highly compressed architecture that we refer to as the ”Shishu-Language-Model”, as depicted in Figure 2. We also extend these methods to the 600M version of the MobileLLM model, to study our hypotheses at a larger scale.

5 EXPERIMENTS

We run most of our experiments on $4 \times$ NVIDIA A100 GPU or $1 \times$ NVIDIA A30 GPU.

Our implementation utilizes HuggingFace Transformers (Wolf et al., 2020) and kernel replacement with FlashAttention 2 (Dao, 2024). Our models are based on the LLaMA architecture (Touvron et al., 2023). We use the Silu activation

Model	HellaSwag	Obqa	WinoGrande	ARC-c	ARC-e	BoolQ	PIQA	Avg.
MobileLLM-125M	28.78	27.4	50.12	22.53	34.81	50.52	59.09	39.03
ShishuLM 125	27.67	26.6	50.04	22.53	33.75	60.73	58.22	39.93
MobileLLM-600M	31.69	27.60	53.91	22.87	38.01	46.39	61.32	40.25
ShishuLM 600	31.25	27.60	53.59	22.53	36.87	60.49	61.37	41.96

Table 1. Zero-shot accuracy of different models (%) on downstream tasks.

Model	Parameters	Validation Perplexity
MobileLLM-125M	124,635,456	16.08
ShishuLM 125	83,921,472	17.86
MobileLLM-600M	603,188,352	13.19
ShishuLM 600	408,506,112	13.73

Table 2. Number of Parameters and validation perplexities.

function (Elfwing et al., 2018) along with rotary position embeddings (RoPE) (Su et al., 2024). We set dropout to 0. We use the AdamW optimizer (Loshchilov & Hutter, 2019) with $\beta_1 = 0.9$ and $\beta_2 = 0.999$, with warmup ratio = 0.05 and weight decay = 5×10^{-3} . The learning rates used for the 83M model (derived from MobileLLM-125M) and for 400M model (derived from MobileLLM-600M) are 1×10^{-3} and 9.5×10^{-4} , respectively, with a cosine scheduler (Loshchilov & Hutter, 2017). The hyperparameters used for the parent models are the same as those for the corresponding derived ones.

For large-scale experiments, we train our models on the first 13B tokens of the SlimPajama dataset (Soboleva et al., 2023). For smaller experiments, we train our models on the Wikitext-103 dataset (Merity et al., 2017) for 3 epochs. We tokenize data using the MobileLLM tokenizers. Since our experiments run on different clusters, we ensure that the effective batch size (the number of samples over which gradients are accumulated, set to 384) remains consistent and accordingly adjust the per-device batch size and gradient accumulation steps. We refer readers to Appendix B for more details on the experiments. We set the block size (sequence length) of an example to 2048 tokens, which leads to processing ≈ 0.78 million tokens in a single step.

Our model weights are initialized from a Normal distribution with mean = 0 and standard deviation = 0.02. We use 1000 examples (roughly 2 million tokens) as the validation set. We also report zero-shot downstream performance on the following tasks: Hellaswag (Zellers et al., 2019), OpenBookQA (Mihaylov et al., 2018), WinoGrande (Sakaguchi et al., 2021), ARC-Easy and ARC-Challenge (Clark et al., 2018), BoolQ (Clark et al., 2019), and PIQA (Bisk et al., 2020), using EleutherAI’s LM EvalHarness framework (Gao et al., 2023).

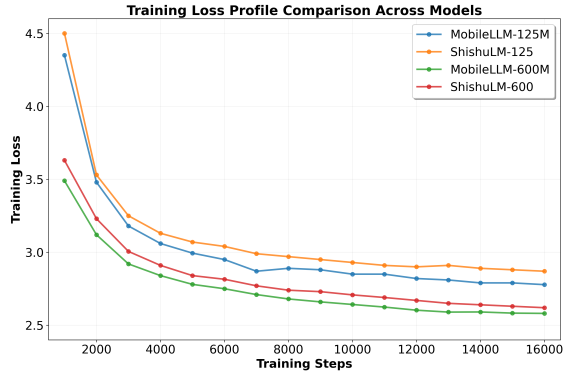


Figure 3. Loss curves for all the model variants.

6 RESULTS

We report our results in this section. For baseline, we train the original MobileLLM-125M and MobileLLM-600M models with same configurations and data as their corresponding ShishuLM models. Please note that in ShishuLM-125 and ShishuLM-600, the numbers 125 and 600 represent the sizes of parent models rather than their own sizes. The actual parameter counts are reported in Table 2. All evaluations in this section are done using a single NVIDIA A30 24G GPU.

6.1 Performance

The loss curves of the both the ShishuLMs are very similar to their parent models as shown in Figure 3. We also report the zero-shot accuracy on downstream tasks in Table 1 along with validation perplexity in Table 2, which show minute loss in performance despite the significantly lesser number of parameters.

6.2 Systems level improvements

We benchmark the all the trained models both at inference (only forward pass) and training (forward + backward pass) on a set of sequence lengths varying from 64 to 2048 tokens, as shown in Tables 3, 4, 5 and 6.

We observe considerable savings both in memory (up to 25%) and latency (up to 40%), with almost similar performance. The memory reduction can be attributed to:

Length	Training (forward + backward)			Inference		
	MobileLLM	ShishuLM	(% reduction)	MobileLLM	ShishuLM	(% reduction)
64	0.0453	0.0706	35.87	0.0187	0.0289	35.46
128	0.0452	0.0773	41.53	0.0188	0.0294	36.09
256	0.0455	0.0747	39.01	0.0188	0.0295	36.41
512	0.0461	0.0751	38.59	0.0188	0.0294	35.99
1024	0.0466	0.0757	38.42	0.0191	0.0301	36.45
2048	0.0512	0.0786	34.81	0.0220	0.0324	31.92
4096	0.0854	0.1316	35.12	0.0300	0.0434	30.95

Table 3. Comparing Training and Inference latency (ms) of MobileLLM-125M and ShishuLM 125.

Length	Training (forward + backward)			Inference		
	MobileLLM	ShishuLM	(% reduction)	MobileLLM	ShishuLM	(% reduction)
64	0.0648	0.0997	35.04	0.0266	0.0381	30.29
128	0.0655	0.1036	36.78	0.0270	0.0397	31.99
256	0.0644	0.0986	34.69	0.0260	0.0386	32.60
512	0.0603	0.0996	39.43	0.0266	0.0387	31.20
1024	0.0848	0.1128	24.81	0.0310	0.0408	24.14
2048	0.1423	0.1885	24.50	0.0486	0.0624	22.03

Table 4. Comparing Training and Inference latency (ms) of MobileLLM-600M and ShishuLM 600.

Length	Training (forward + backward)			Inference		
	MobileLLM	ShishuLM	(% reduction)	MobileLLM	ShishuLM	(% reduction)
64	0.5611	0.6855	18.16	0.2559	0.3085	17.04
128	0.6754	0.8013	15.71	0.3072	0.3713	17.27
256	0.9049	1.0746	15.79	0.4097	0.4949	17.22
512	1.3924	1.6606	16.15	0.6183	0.7530	17.89
1024	2.3951	2.8323	15.44	1.0355	1.2525	17.32
2048	4.3226	5.1196	15.57	1.8423	2.2363	17.62

Table 5. Comparing Training and Inference memory (GB) of MobileLLM-125M and ShishuLM 125.

Length	Training (forward + backward)			Inference		
	MobileLLM	ShishuLM	(% reduction)	MobileLLM	ShishuLM	(% reduction)
64	2.0448	2.6959	24.15	0.9813	1.3030	24.69
128	2.3053	2.9896	22.89	1.1054	1.4477	23.65
256	2.8806	3.6496	21.07	1.3806	1.7668	21.86
512	3.9409	4.8753	19.17	1.8883	2.3567	19.88
1024	6.0206	7.2982	17.51	2.8512	3.4868	18.23
2048	10.3252	12.3376	16.31	4.8314	5.8189	16.97

Table 6. Comparing Training and Inference Memory (GB) of MobileLLM-600M and ShishuLM 600.

- Reduced number of parameters : this saves the model size as well as the memory associated with backpropagation.
- Removal of attention layers in the later layers reduces the KV Cache size and this saving is more pronounced with increasing sequence length.

The latency improvement comes solely from the reduction in self-attention computation, as the remaining compute units are maintained as is.

7 CONCLUSION

We proposed ShishuLM, an efficient architecture for training language models by identifying redundancy in attention modules in the later layers of existing architectures. We demonstrated that similar performance can be achieved by pre-training without these layers. We identified similarity in weight distributions in consecutive layers and share weights in the MLP-only blocks to further optimize our models. This work is agnostic to any error-based feedback mechanisms and is based on results from interpretability research. Along with memory saving achieved from reducing parameters, eliminating attention layers reduces quadratic computational units and decreases the KV cache size. Moreover, these benefits can be leveraged during both training and inference. We believe that our findings will provide directions for future research for developing parameter-efficient architectures that fully utilize their computational capacity and enabling the training of smaller yet equally effective models. With additional computational resources, systematic hyperparameter tuning could yield substantial improvements in the performance of our models.

8 LIMITATIONS

A drawback of this work is that we were unable to scale our results to larger models due to limited compute resources. To address this issue, we have plotted the loss curves of both the original model and the corresponding ShishuLM. Furthermore, our insights and quantification are specific to the LLaMA architecture.

9 DIRECTIONS FOR FUTURE WORK

Although our experiments show that roughly $1/3^{rd}$ of the initial decoder blocks containing attention is sufficient, we leave a theoretical quantification of this number for future work. Another interesting line of work would be to see how these methods extend to different model architectures such as Qwen (Bai et al., 2023), where previous research has seen different behavior in terms of layer redundancy as compared to the LLaMA architecture (Gromov et al., 2025).

REFERENCES

- Ainslie, J., Lee-Thorp, J., de Jong, M., Zemlyanskiy, Y., Lebron, F., and Sanghai, S. GQA: Training generalized multi-query transformer models from multi-head checkpoints. In Bouamor, H., Pino, J., and Bali, K. (eds.), *Proceedings of the 2023 Conference on Empirical Methods in Natural Language Processing*, pp. 4895–4901, Singapore, December 2023. Association for Computational Linguistics. doi: 10.18653/v1/2023.emnlp-main.298. URL <https://aclanthology.org/2023.emnlp-main.298/>.
- Artzy, A. B. and Schwartz, R. Attend first, consolidate later: On the importance of attention in different LLM layers. In Belinkov, Y., Kim, N., Jumelet, J., Mohebbi, H., Mueller, A., and Chen, H. (eds.), *Proceedings of the 7th BlackboxNLP Workshop: Analyzing and Interpreting Neural Networks for NLP*, pp. 177–184, Miami, Florida, US, November 2024. Association for Computational Linguistics. doi: 10.18653/v1/2024.blackboxnlp-1.10. URL <https://aclanthology.org/2024.blackboxnlp-1.10/>.
- Ashkboos, S., Croci, M. L., do Nascimento, M. G., Hoefler, T., and Hensman, J. SliceGPT: Compress large language models by deleting rows and columns. In *The Twelfth International Conference on Learning Representations*, 2024. URL <https://openreview.net/forum?id=vXxardq6db>.
- Bai, J., Bai, S., Chu, Y., Cui, Z., Dang, K., Deng, X., Fan, Y., Ge, W., Han, Y., Huang, F., Hui, B., Ji, L., Li, M., Lin, J., Lin, R., Liu, D., Liu, G., Lu, C., Lu, K., Ma, J., Men, R., Ren, X., Ren, X., Tan, C., Tan, S., Tu, J., Wang, P., Wang, S., Wang, W., Wu, S., Xu, B., Xu, J., Yang, A., Yang, H., Yang, J., Yang, S., Yao, Y., Yu, B., Yuan, H., Yuan, Z., Zhang, J., Zhang, X., Zhang, Y., Zhang, Z., Zhou, C., Zhou, J., Zhou, X., and Zhu, T. Qwen technical report, 2023. URL <https://arxiv.org/abs/2309.16609>.
- Bisk, Y., Zellers, R., Le bras, R., Gao, J., and Choi, Y. Piqa: Reasoning about physical commonsense in natural language. *Proceedings of the AAAI Conference on Artificial Intelligence*, 34(05):7432–7439, Apr. 2020. doi: 10.1609/aaai.v34i05.6239. URL <https://ojs.aaai.org/index.php/AAAI/article/view/6239>.
- Brandon, W., Mishra, M., Nrusimha, A., Panda, R., and Ragan-Kelley, J. Reducing transformer key-value cache size with cross-layer attention. In *The Thirty-eighth Annual Conference on Neural Information Processing Systems*, 2024. URL <https://openreview.net/forum?id=M2UzLRoqic>.

- Clark, C., Lee, K., Chang, M.-W., Kwiatkowski, T., Collins, M., and Toutanova, K. BoolQ: Exploring the surprising difficulty of natural yes/no questions. In Burstein, J., Doran, C., and Solorio, T. (eds.), *Proceedings of the 2019 Conference of the North American Chapter of the Association for Computational Linguistics: Human Language Technologies, Volume 1 (Long and Short Papers)*, pp. 2924–2936, Minneapolis, Minnesota, June 2019. Association for Computational Linguistics. doi: 10.18653/v1/N19-1300. URL <https://aclanthology.org/N19-1300/>.
- Clark, P., Cowhey, I., Etzioni, O., Khot, T., Sabharwal, A., Schoenick, C., and Taffjord, O. Think you have solved question answering? try arc, the ai2 reasoning challenge, 2018. URL <https://arxiv.org/abs/1803.05457>.
- Dao, T. Flashattention-2: Faster attention with better parallelism and work partitioning. In *The Twelfth International Conference on Learning Representations*, 2024. URL <https://openreview.net/forum?id=mZn2Xyh9Ec>.
- Elfwing, S., Uchibe, E., and Doya, K. Sigmoid-weighted linear units for neural network function approximation in reinforcement learning. *Neural Networks*, 107:3–11, 2018. ISSN 0893-6080. doi: <https://doi.org/10.1016/j.neunet.2017.12.012>. URL <https://www.sciencedirect.com/science/article/pii/S0893608017302976>. Special issue on deep reinforcement learning.
- Frantar, E. and Alistarh, D. SparseGPT: Massive language models can be accurately pruned in one-shot. In Krause, A., Brunskill, E., Cho, K., Engelhardt, B., Sabato, S., and Scarlett, J. (eds.), *Proceedings of the 40th International Conference on Machine Learning*, volume 202 of *Proceedings of Machine Learning Research*, pp. 10323–10337. PMLR, 23–29 Jul 2023. URL <https://proceedings.mlr.press/v202/frantar23a.html>.
- Gao, L., Tow, J., Abbasi, B., Biderman, S., Black, S., DiPofi, A., Foster, C., Golding, L., Hsu, J., Le Noac’h, A., Li, H., McDonnell, K., Muennighoff, N., Ociepa, C., Phang, J., Reynolds, L., Schoelkopf, H., Skowron, A., Sutawika, L., Tang, E., Thite, A., Wang, B., Wang, K., and Zou, A. A framework for few-shot language model evaluation, 12 2023. URL <https://zenodo.org/records/10256836>.
- Gromov, A., Tirumala, K., Shapourian, H., Glorioso, P., and Roberts, D. The unreasonable ineffectiveness of the deeper layers. In *The Thirteenth International Conference on Learning Representations*, 2025. URL <https://openreview.net/forum?id=ngmEcEer8a>.
- Gu, A. and Dao, T. Mamba: Linear-time sequence modeling with selective state spaces. In *First Conference on Language Modeling*, 2024. URL <https://openreview.net/forum?id=tEYskw1VY2>.
- Hubara, I., Courbariaux, M., Soudry, D., El-Yaniv, R., and Bengio, Y. Quantized neural networks: training neural networks with low precision weights and activations. *J. Mach. Learn. Res.*, 18(1):6869–6898, January 2017. ISSN 1532-4435.
- Javaheripi, M., Bubeck, S., Abdin, M., Aneja, J., Bubeck, S., Mendes, C. C. T., Chen, W., Del Giorno, A., Eldan, R., Gopi, S., et al. Phi-2: The surprising power of small language models. *Microsoft Research Blog*, 2023.
- Jiang, A. Q., Sablayrolles, A., Mensch, A., Bamford, C., Chaplot, D. S., de las Casas, D., Bressand, F., Lengyel, G., Lample, G., Saulnier, L., Lavaud, L. R., Lachaux, M.-A., Stock, P., Scao, T. L., Lavril, T., Wang, T., Lacroix, T., and Sayed, W. E. Mistral 7b, 2023. URL <https://arxiv.org/abs/2310.06825>.
- Kaddour, J. The minipile challenge for data-efficient language models, 2023. URL <https://arxiv.org/abs/2304.08442>.
- Katharopoulos, A., Vyas, A., Pappas, N., and Fleuret, F. Transformers are rnns: fast autoregressive transformers with linear attention. In *Proceedings of the 37th International Conference on Machine Learning*, ICML’20. JMLR.org, 2020.
- Lad, V., Gurnee, W., and Tegmark, M. The remarkable robustness of LLMs: Stages of inference? In *ICML 2024 Workshop on Mechanistic Interpretability*, 2024. URL <https://openreview.net/forum?id=R5unwb9KPc>.
- Liu, Z., Zhao, C., Iandola, F., Lai, C., Tian, Y., Fedorov, I., Xiong, Y., Chang, E., Shi, Y., Krishnamoorthi, R., Lai, L., and Chandra, V. Mobilellm: optimizing sub-billion parameter language models for on-device use cases. In *Proceedings of the 41st International Conference on Machine Learning*, ICML’24. JMLR.org, 2024.
- Loshchilov, I. and Hutter, F. SGDR: Stochastic gradient descent with warm restarts. In *International Conference on Learning Representations*, 2017. URL <https://openreview.net/forum?id=Skq89Scxx>.
- Loshchilov, I. and Hutter, F. Decoupled weight decay regularization. In *International Conference on Learning Representations*, 2019. URL <https://openreview.net/forum?id=Bkg6RiCqY7>.

- Ma, X., Fang, G., and Wang, X. Llm-pruner: On the structural pruning of large language models. In Oh, A., Nauermann, T., Globerson, A., Saenko, K., Hardt, M., and Levine, S. (eds.), *Advances in Neural Information Processing Systems*, volume 36, pp. 21702–21720. Curran Associates, Inc., 2023.
- Men, X., Xu, M., Zhang, Q., Wang, B., Lin, H., Lu, Y., Han, X., and Chen, W. Shortgpt: Layers in large language models are more redundant than you expect, 2024. URL <https://arxiv.org/abs/2403.03853>.
- Merity, S., Xiong, C., Bradbury, J., and Socher, R. Pointer sentinel mixture models. In *International Conference on Learning Representations*, 2017. URL <https://openreview.net/forum?id=Byj72udxe>.
- Mihaylov, T., Clark, P., Khot, T., and Sabharwal, A. Can a suit of armor conduct electricity? a new dataset for open book question answering. In Riloff, E., Chiang, D., Hockenmaier, J., and Tsujii, J. (eds.), *Proceedings of the 2018 Conference on Empirical Methods in Natural Language Processing*, pp. 2381–2391, Brussels, Belgium, October–November 2018. Association for Computational Linguistics. doi: 10.18653/v1/D18-1260. URL <https://aclanthology.org/D18-1260/>.
- Mishra, A., Latorre, J. A., Pool, J., Stosic, D., Stosic, D., Venkatesh, G., Yu, C., and Micikevicius, P. Accelerating sparse deep neural networks, 2021. URL <https://arxiv.org/abs/2104.08378>.
- Rajput, S., Sheng, Y., Owen, S., and Chiley, V. Inference-friendly models with MixAttention. In Rezagholizadeh, M., Passban, P., Samiee, S., Partovi Nia, V., Cheng, Y., Deng, Y., Liu, Q., and Chen, B. (eds.), *Proceedings of The 4th NeurIPS Efficient Natural Language and Speech Processing Workshop*, volume 262 of *Proceedings of Machine Learning Research*, pp. 370–381. PMLR, 14 Dec 2024. URL <https://proceedings.mlr.press/v262/rajput24a.html>.
- Ro, Y., Zhang, Z., Kundu, S., Wang, Z., and Akella, A. On-the-fly adaptive distillation of transformer to dual-state linear attention for long-context LLM serving. In *Forty-second International Conference on Machine Learning*, 2025. URL <https://openreview.net/forum?id=pqHWzviKKN>.
- Rubner, Y., Tomasi, C., and Guibas, L. A metric for distributions with applications to image databases. In *Sixth International Conference on Computer Vision (IEEE Cat. No.98CH36271)*, pp. 59–66, 1998. doi: 10.1109/ICCV.1998.710701.
- Sakaguchi, K., Bras, R. L., Bhagavatula, C., and Choi, Y. Winogrande: an adversarial winograd schema challenge at scale. *Commun. ACM*, 64(9):99–106, August 2021. ISSN 0001-0782. doi: 10.1145/3474381. URL <https://doi.org/10.1145/3474381>.
- Siddiqui, S. A., Dong, X., Heinrich, G., Breuel, T., Kautz, J., Krueger, D., and Molchanov, P. A deeper look at depth pruning of LLMs. In *ICML 2024 Workshop on Theoretical Foundations of Foundation Models*, 2024. URL <https://openreview.net/forum?id=9B7ayWclwN>.
- Soboleva, D., Al-Khateeb, F., Myers, R., Steeves, J. R., Hestness, J., and Dey, N. SlimPajama: A 627B token cleaned and deduplicated version of RedPajama, 2023.
- Song, J., Oh, K., Kim, T., Kim, H., Kim, Y., and Kim, J.-J. Sleb: streamlining llms through redundancy verification and elimination of transformer blocks. In *Proceedings of the 41st International Conference on Machine Learning, ICML’24*. JMLR.org, 2024.
- Su, J., Lu, Y., Pan, S., Murtadha, A., Wen, B., and Liu, Y. Roformer: Enhanced transformer with rotary position embedding. *Neurocomputing*, 568:127063, 2024.
- Sun, M., Liu, Z., Bair, A., and Kolter, J. Z. A simple and effective pruning approach for large language models. In *The Twelfth International Conference on Learning Representations*, 2024a. URL <https://openreview.net/forum?id=PxoFut3dWW>.
- Sun, Y., Dong, L., Zhu, Y., Huang, S., Wang, W., Ma, S., Zhang, Q., Wang, J., and Wei, F. You only cache once: Decoder-decoder architectures for language models. In Globerson, A., Mackey, L., Belgrave, D., Fan, A., Paquet, U., Tomczak, J., and Zhang, C. (eds.), *Advances in Neural Information Processing Systems*, volume 37, pp. 7339–7361. Curran Associates, Inc., 2024b.
- Touvron, H., Lavril, T., Izacard, G., Martinet, X., Lachaux, M.-A., Lacroix, T., Rozière, B., Goyal, N., Hambro, E., Azhar, F., Rodriguez, A., Joulin, A., Grave, E., and Lample, G. Llama: Open and efficient foundation language models, 2023. URL <https://arxiv.org/abs/2302.13971>.
- Vaswani, A., Shazeer, N., Parmar, N., Uszkoreit, J., Jones, L., Gomez, A. N., Kaiser, L., and Polosukhin, I. Attention is all you need. In *Proceedings of the 31st International Conference on Neural Information Processing Systems, NIPS’17*, pp. 6000–6010, 2017.
- Wolf, T., Debut, L., Sanh, V., Chaumond, J., Delangue, C., Moi, A., Cistac, P., Rault, T., Louf, R., Funtowicz, M., Davison, J., Shleifer, S., von Platen, P., Ma, C., Jernite, Y., Plu, J., Xu, C., Le Scao, T., Gugger, S., Drame, M., Lhoest, Q., and Rush, A. Transformers:

State-of-the-art natural language processing. In Liu, Q. and Schlangen, D. (eds.), *Proceedings of the 2020 Conference on Empirical Methods in Natural Language Processing: System Demonstrations*, pp. 38–45, Online, October 2020. Association for Computational Linguistics. doi: 10.18653/v1/2020.emnlp-demos.6. URL <https://aclanthology.org/2020.emnlp-demos.6/>.

Wu, H. and Tu, K. Layer-condensed KV cache for efficient inference of large language models. In Ku, L.-W., Martins, A., and Srikumar, V. (eds.), *Proceedings of the 62nd Annual Meeting of the Association for Computational Linguistics (Volume 1: Long Papers)*, pp. 11175–11188, Bangkok, Thailand, August 2024. Association for Computational Linguistics. doi: 10.18653/v1/2024.acl-long.602. URL <https://aclanthology.org/2024.acl-long.602/>.

Yang, S., Wang, B., Shen, Y., Panda, R., and Kim, Y. Gated linear attention transformers with hardware-efficient training. In *Proceedings of the 41st International Conference on Machine Learning, ICML’24*. JMLR.org, 2024a.

Yang, Y., Cao, Z., and Zhao, H. LaCo: Large language model pruning via layer collapse. In Al-Onaizan, Y., Bansal, M., and Chen, Y.-N. (eds.), *Findings of the Association for Computational Linguistics: EMNLP 2024*, pp. 6401–6417, Miami, Florida, USA, November 2024b. Association for Computational Linguistics. doi: 10.18653/v1/2024.findings-emnlp.372. URL <https://aclanthology.org/2024.findings-emnlp.372/>.

Zellers, R., Holtzman, A., Bisk, Y., Farhadi, A., and Choi, Y. HellaSwag: Can a machine really finish your sentence? In Korhonen, A., Traum, D., and Márquez, L. (eds.), *Proceedings of the 57th Annual Meeting of the Association for Computational Linguistics*, pp. 4791–4800, Florence, Italy, July 2019. Association for Computational Linguistics. doi: 10.18653/v1/P19-1472. URL <https://aclanthology.org/P19-1472/>.

A PROOF FOR EQUATION 3

Let γ and β denote the affine parameters of the post-attention normalization layer, and for an input x , let μ_x and σ_x denote its mean and standard deviation, respectively. Let ϵ be a small parameter included for numerical stability. We may write:

$$LN(x) = \gamma \frac{x - \mu_x}{\sqrt{\sigma_x^2 + \epsilon}} + \beta$$

The mean μ_1 of αx is $\alpha \mu_x$ and the standard deviation σ_1 is

$\alpha \sigma_x$.

$$LN(\alpha x) = \gamma \frac{\alpha x - \mu_1}{\sqrt{\sigma_1^2 + \epsilon}} + \beta \tag{4}$$

$$= \gamma \frac{\alpha(x - \mu_x)}{\sqrt{\alpha^2 \sigma_x^2 + \epsilon}} + \beta \tag{5}$$

$$\approx \gamma \frac{x - \mu_x}{\sqrt{\sigma_x^2 + \epsilon}} + \beta \tag{6}$$

$$\approx LN(x) \tag{7}$$

Note that the LLaMA architecture (Touvron et al., 2023) as used in this paper uses RMSNorm, which avoids mean subtraction and scales by the Root Mean Squared instead of the standard deviation. Therefore for input x with dimension n ,

$$LN_{RMS}(x) = \frac{x}{\sqrt{(\sum_{i=1}^n x_i^2) + \epsilon}}$$

$$LN_{RMS}(\alpha x) = \frac{\alpha x}{\sqrt{(\alpha^2 \sum_{i=1}^n x_i^2) + \epsilon}} \tag{8}$$

$$\approx \frac{x}{\sqrt{(\sum_{i=1}^n x_i^2) + \epsilon}} \tag{9}$$

$$= LN_{RMS}(x) \tag{10}$$

B DETAILS OF EXPERIMENTS

Following Wu & Tu we provide the model configurations and training details in table 7.

C ATTENTION LINEARITY

In this section we show our results for the linearity in the computation of the input normalization + self attention layers. We give prefill inputs with 54, 118, 246 and 502 tokens and allow the model to generate 10 tokens.

1. The input-output pairs per layer are fed to a linear model and the Mean Squared Error is shown in Figure 7.
2. The cosine similarity values between the input and output per layer for the generated tokens are averaged and shown in Figure 11
3. The L_2 distance between the matrix found in 1 and the nearest scalar matrix (i.e., of the form αI) is shown in Figure 15.

Model	ShishuLM 125	MobileLLM-125M	ShishuLM 600	MobileLLM-600M
Hidden Size	576	576	1152	1152
Intermediate Size	1536	1536	3072	3072
# Layers	30	30	43	40
# Decoder Layers	10	30	13	40
# ShishuMLP Layers	10*2	–	15*2	–
# Attention Heads	9	9	18	18
# KV Heads	3	3	6	6
RMS Norm eps			1e-5	
Vocab Size			32000	
GPUs	1x A30	3x A100	4x A100	4x A100
Per device batch-size	16	64	16	16

Table 7. Model configurations and training details

D MLP WEIGHT DISTRIBUTION SIMILARITY

The heatmaps of similarity measured (using the Earth Mover’s distance) between the distribution of weights across the MLP layers in MobileLLM-125M and MobileLLM-600M are shown in figures 16 and 17 respectively. The exact r_{max} scores as described in the Methodology Section are given in table 8

Model	gate_proj	up_proj	down_proj
MobileLLM-125M	0.2845	0.6236	0.4956
MobileLLM-350M	0.2272	0.1689	0.1387
MobileLLM-600M	0.1911	0.2097	0.1025

Table 8. $r_{max} * 100$ for distribution of weights across MLP layers

E ABLATION STUDY ON ATTENTION BUDGET

In this section we give a summary of our experimental results on quantifying attention budget. Table 9 shows the result of sequentially removing attention layers from the top and pretraining. With $1/3^{rd}$ attention budget, we check whether placing some of the attention layers at the top is beneficial, since this would lead to attending tokens with refined representations. This is shown in Table 10.

Pre-training is done on the WikiText-103 (Merity et al., 2017) for 3 epochs with learning rate, weight decay and warmup ratio being 1×10^{-3} , 5×10^{-2} and 0.05 respectively. All experiments in this section are done using a single NVIDIA A100 GPU with batch size = 64 and block size = 1024.

Architecture	Training loss	Validation loss	Perplexity
30 + 0	2.99	2.60	13.42
25 + 5	3.01	2.60	13.42
20+10	2.98	2.59	13.37
15+15	2.96	2.58	13.20
10+20	2.97	2.60	13.42
8 + 22	2.99	2.62	13.71
6 + 24	3.01	2.63	13.93
4 + 26	3.05	2.67	14.51

Table 9. Losses and validation perplexity for different attention budgets. $n+m$ means n decoder layers followed by m ShishuMLP layers

Architecture	Training loss	Validation loss	Perplexity
0 + 10	3.08	2.71	15.09
2 + 8	3.02	2.64	13.98
4 + 6	2.99	2.61	13.60
6 + 4	3.01	2.62	13.78
8 + 2	2.98	2.61	13.61
10 + 0	2.97	2.60	13.42

Table 10. Losses and validation perplexity for different attention budgets. $n + m$ means n decoder layers at the bottom and m decoder layers at the top along with weight shared ShishuMLP layers stacked in between.

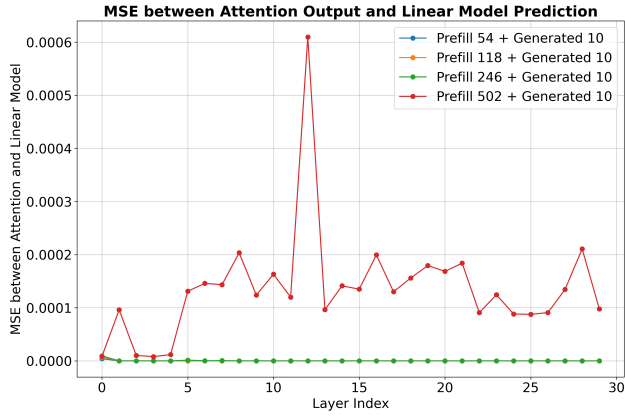


Figure 4. MobileLLM-125M

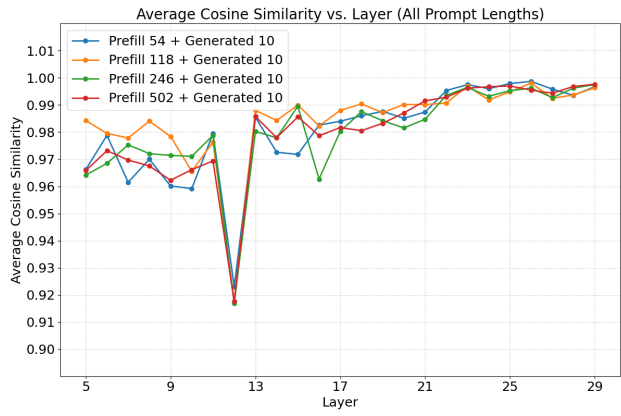


Figure 8. MobileLLM-125M

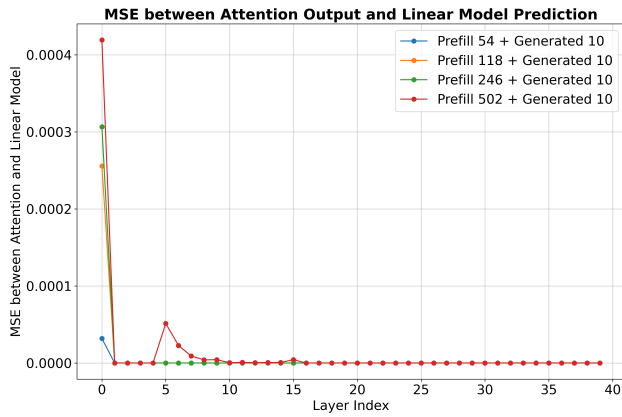


Figure 5. MobileLLM-600M

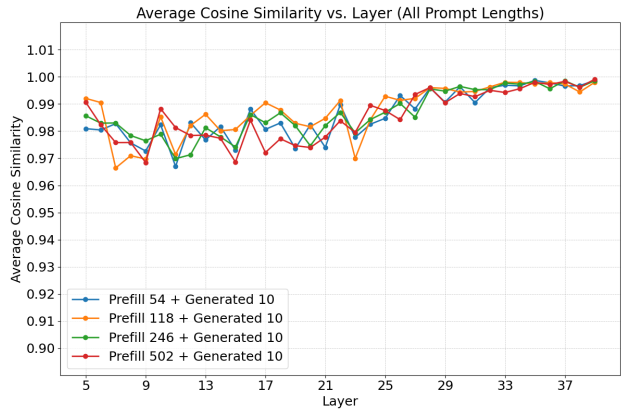


Figure 9. MobileLLM-600M

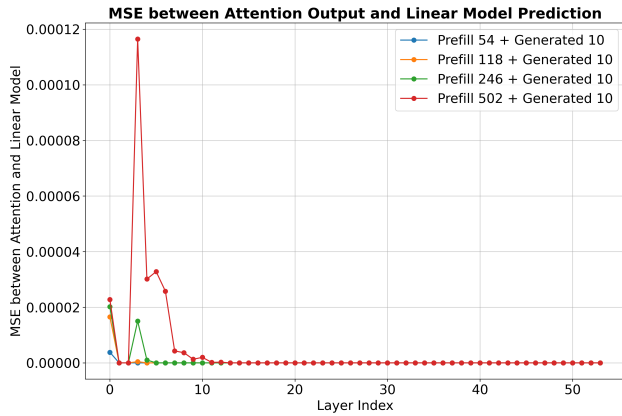


Figure 6. MobileLLM-1.5B

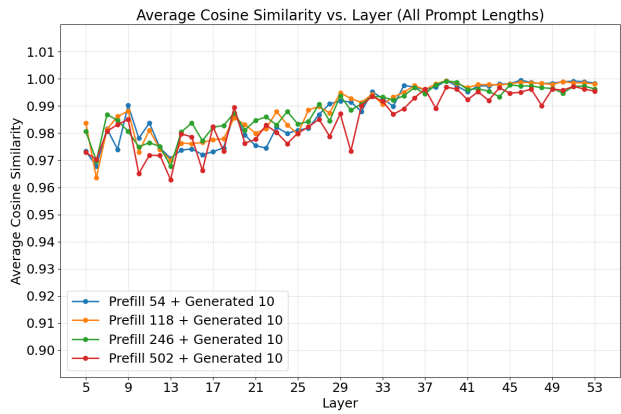


Figure 10. MobileLLM-1.5B

Figure 7. Mean squared error for fitting a linear layer in place of input normalisation + self-attention

Figure 11. Average cosine similarity in generated tokens

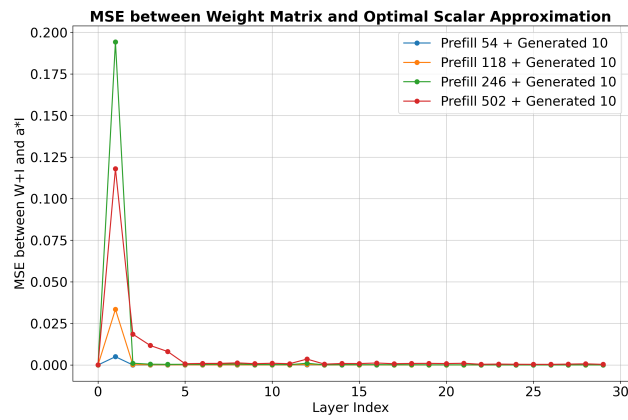


Figure 12. MobileLLM-125M

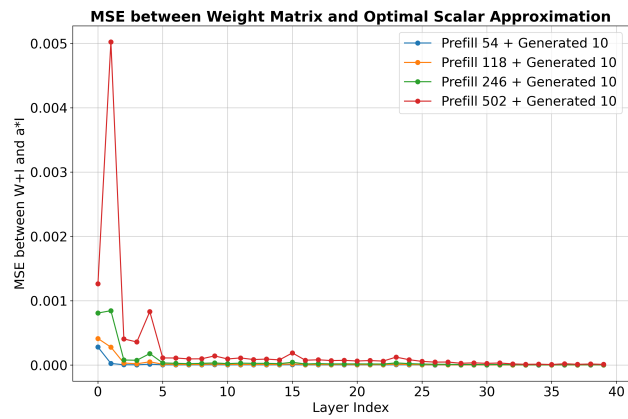


Figure 13. MobileLLM-600M

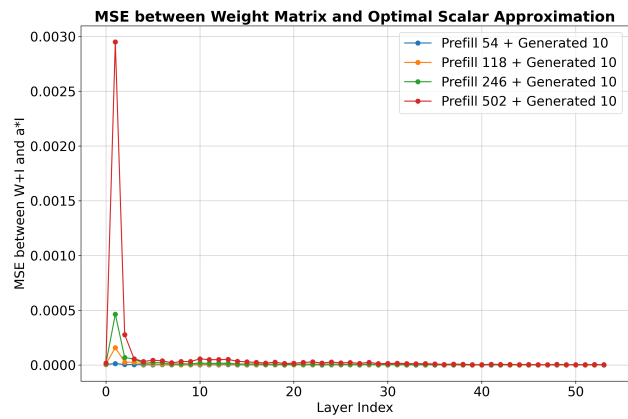


Figure 14. MobileLLM-1.5B

Figure 15. MSE values for fitting αI to Attention Computation

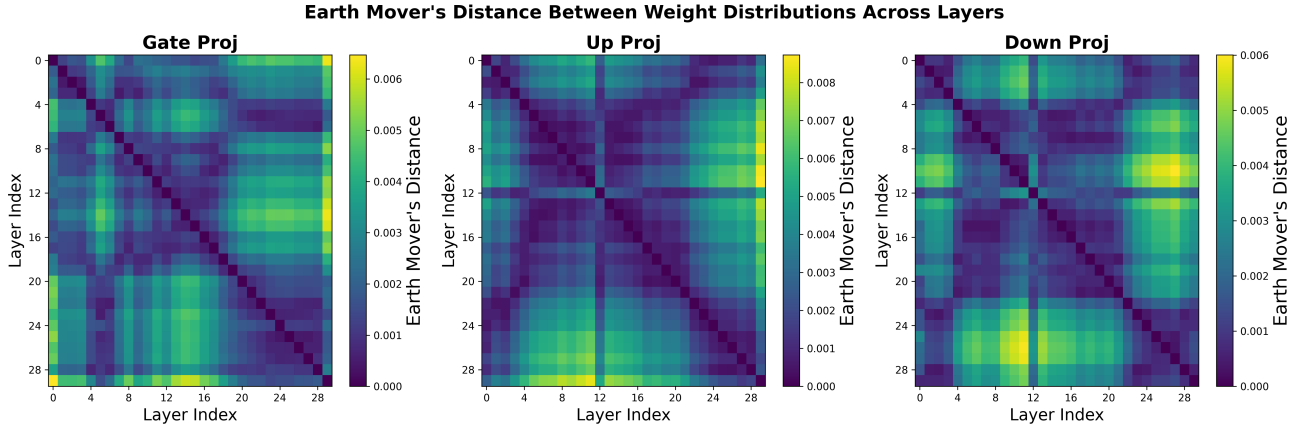


Figure 16.

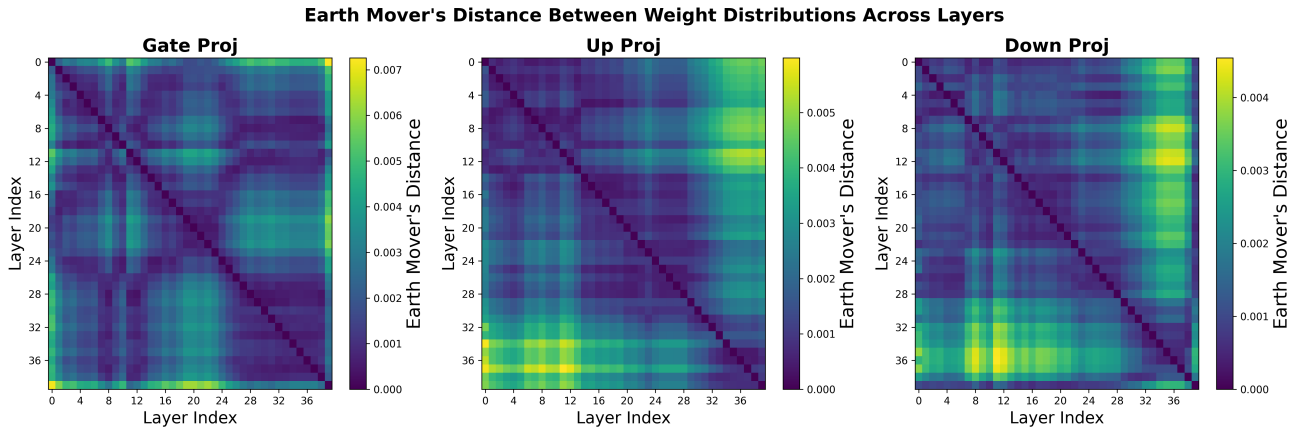


Figure 17.